JOURNAL OF VIROLOGY, Apr. 2008, p. 4091–4101 Vol. 82, No. 8
0022-538X/08/$08.00+0 doi:10.1128/JVI.02552-07

$CD4^+$ Target Cell Availability Determines the Dynamics of Immune Escape and Reversion In Vivo[▽]

Janka Petravic,[1] Liyen Loh,[2] Stephen J. Kent,[2] and Miles P. Davenport[1]*

Complex Systems in Biology Group, Centre for Vascular Research, University of NSW, Kensington, NSW 2052, Australia,[1] and Department of Microbiology and Immunology, University of Melbourne, Melbourne 3010, Australia[2]

Received 29 November 2007/Accepted 30 January 2008

Infections with human immunodeficiency virus (HIV) and the closely related monkey viruses simian-human immunodeficiency virus (SHIV) and simian immunodeficiency virus (SIV) are characterized by progressive waves of immune responses, followed by viral mutation and "immune escape." However, escape mutation usually leads to lower replicative fitness, and in the absence of immune pressure, an escape mutant (EM) virus "reverts" to the wild-type phenotype. Analysis of the dynamics of immune escape and reversion has suggested it is a mechanism for identifying the immunogens best capable of controlling viremia. We have analyzed and modeled data of the dynamics of wild-type (WT) and EM viruses during SHIV infection of macaques. Modeling suggests that the dynamics of reversion and immune escape should be determined by the availability of target cells for infection. Consistent with this suggestion, we find that the rate of reversion of cytotoxic T-lymphocyte (CTL) EM virus strongly correlates with the number of $CD4^+$ T cells available for infection. This phenomenon also affects the rate of immune escape, since this rate is determined by the balance of CTL killing and the WT fitness advantage. This analysis predicts that the optimal timing for the selection of immune escape variants will be immediately after the peak of viremia and that the development of escape variants at later times will lead to slower selection. This has important implications for comparative studies of immune escape and reversion in different infections and for identifying epitopes with high fitness cost for use as vaccine targets.

Human immunodeficiency virus (HIV) has a high mutation rate, leading to the rapid accumulation of viral variants during infection. The immune response exerts a selective pressure on the virus, leading to the outgrowth of viral variants that have a reduced or no immune recognition. The selection of an escape mutant (EM) virus has been observed for humoral (34, 36) and $CD4^+$ (19) and $CD8^+$ (9, 32) T-cell recognition of the virus. The sequential escape from immune response contributes to the clinical progression of the infection over time (18), and at a population level, an increased number of escape mutations is associated with a more advanced disease stage (5). However, the viral mutations that lead to the loss of immune recognition may also impair the viral replicative capacity, the "fitness cost" of an escape mutation. In the absence of immune pressure, the advantage of the EM virus (i.e., reduced immune recognition) is lost, and the reduced replicative capacity of EM virus compared to that of the wild-type (WT) virus leads to a reversion from the EM to the WT virus. This has been observed in vitro (15, 27), as well as in both humans and macaques who lack the major histocompatibility complex (MHC) molecules required for the recognition of the WT epitope (10, 14, 22). A phase of transient reversion followed by reescape has also been observed early after infection in individuals bearing the required MHC, as at least some growth of the WT virus is required to induce an immune response to the epitope (1, 10). This dynamic of immune escape and reversion within the infected individual leads to the transmission and persistence of both WT and EM virus in the human population (28).

The ability of HIV to escape immune recognition presents a significant problem for vaccine design, as vaccine efficacy may be compromised by the rapid selection of EM virus. The ideal vaccine may be one that targets immunogenic but highly conserved regions of the virus, where immune escape is not possible. However, in the absence of such invariant epitopes, the ideal vaccine targets may be multiple epitopes where immune escape leads to a very high fitness cost to the virus (17, 21). Thus, immune escape, if it occurs, will lead to a crippled virus with reduced pathogenic potential. One method for estimating the fitness cost of escape mutation is to measure the rate of reversion from EM to WT during infection (11, 21). Thus, EM virus that reverts extremely rapidly is assumed to do so because of significantly impaired replicative capacity compared to WT virus. An EM virus that reverts slowly is assumed to have little or no fitness cost. If an EM virus has no fitness cost relative to that of the wild type, it should eventually spread within the host population to become the consensus sequence.

Studies of the rate of immune escape suggest that escape can be completed extremely rapidly in acute infection, and may be significantly slower during chronic infection (2, 24). This appears due most likely to the peak of immune response observed in the first few weeks after infection. The rate of reversion from EM to WT virus also appears to be rapid if it occurs early during infection but slower if it occurs

* Corresponding author. Mailing address: Complex Systems in Biology Group, Centre for Vascular Research, University of New South Wales, Kensington, NSW 2052, Australia. Phone: 61 2 93852762. Fax: 61 2 93851389. E-mail: m.davenport@unsw.edu.au.

▽ Published ahead of print on 13 February 2008.

later in disease (24). Thus, the time at which the competition between EM and WT virus occurs appears to be an important determinant of the rate of selection and is an important consideration in comparing the rates of escape and reversion between different infection models or between different epitopes. In particular, in some circumstances, both WT and EM virus may be present and begin competing from the time of infection, and thus the rates of escape and reversion can be measured during acute infection. However, in many circumstances (and most likely in natural infection), there may be a delay before one variant arises from the other due to mutation. If the strength of the selection wanes with time, then the observed rate of selection will be intimately linked with the time at which the mutant first arises (24).

Cytotoxic T lymphocytes (CTLs) kill infected target cells, and we hypothesized that target cell availability could be a crucial variable affecting the rates of immune escape and reversion. Here, we apply a mathematical modeling approach to clarify how the underlying virus and target ($CD4^+$ T lymphocyte) cell dynamics cause the time dependence of reversion and escape rates. We then compare these model predictions with the dynamics of reversion and escape observed in vivo using a recently reported real-time PCR-based assay for measuring the absolute levels of EM and WT variants in simian-human immunodeficiency virus (SHIV) infection of macaques. Although X4-tropic SHIV differs from HIV in the range of $CD4^+$ T cells available for infection, the X4-tropic SHIV has an advantage in its target cell pool being known and measurable at all times.

We find that the rate of reversion is directly proportional to the number of available uninfected $CD4^+$ T-cell targets. Thus, animals have a high reversion rate immediately after infection, due to a high basic fitness cost at normal CD4 T-cell levels. However, this maximal reversion rate declines substantially as $CD4^+$ T cells are depleted. As a consequence, the effective fitness cost of the EM virus declines rapidly over the course of infection, leading to the reduced reversion rate observed at later stages of infection. Since the rate of escape is the balance of immune pressure and the effective fitness cost at any time, this has important implications for the dynamics of immune escape and control in vivo.

MATERIALS AND METHODS

In vivo studies. The experimental studies of viral loads of EM and wild-type virus have been published previously (23). Briefly, we studied pigtail macaques (*Macaca nemestrina*) infected with the CXCR4-tropic SHIV ($SHIV_{mn229}$) virus. The $SHIV_{mn229}$ stock is composed of ~90% of the K165R SIV Gag mutation, which escapes the immunodominant *Mane-A*10*$^+$ restricted KP9-specific $CD8^+$ CTL epitope. We studied eight animals in detail, where we had frequent measurements of KP9-specific T cells, EM and WT viral loads, and $CD4^+$ T cells. Four animals were *Mane-A*10* negative (4194, 4301, H20, and 1.1705) and used to study reversion of the EM KP9 to the WT, and four animals were *Mane-A*10* positive (6167, 5712, 5614, and 6276) and used to study transient reversion and reescape at KP9. Two of these four *Mane-A*10*$^+$ macaques had received T-cell-based vaccines (animal 6276 received DNA prime and fowlpox virus [DNA/FPV] boost vaccines; animal 5614 received DNA vaccines only) prior to the SHIV challenge. We chose vaccinated and control animals in order to assess the impact of prior induction of KP9-specific $CD8^+$ T cells on escape rates. The dynamics of the EM and WT viruses at the SIV Gag KP9 epitope were measured by using a novel quantitative real-time PCR assay as reported recently (24). $CD4^+$ T-cell counts and the number of KP9-specific $CD8^+$ T cells (detected using KP9/*Mane-A*10* tetramers) were measured by flow cytometry (6, 8).

A simple model of reversion. The simplest model of reversion is based on the basic model of virus dynamics, with the wild-type (W) and EM (M) viruses competing for infection of target cells

$$\frac{dI_W}{dt} = k_W W T - \delta I_W \tag{1}$$

$$\frac{dI_M}{dt} = k_M M T - \delta I_M$$

$$\frac{dW}{dt} = p_W I_W - c_W W$$

$$\frac{dM}{dt} = p_M I_M - c_M M$$

In equation 1, T is the (time-varying) number of uninfected $CD4^+$ T cells that are targets for infection by the virus. It represents the common environment in which both strains grow. I_W and I_M are the cells infected by the WT and EM viruses, respectively. The infectivity values k_W and k_M characterize the rate of infection of target cells by WT or EM virus, and δ is the death rate of infected cells. We assume that WT and EM sequences differ only in one epitope. In the absence of immune recognition of the epitope, the infected cells from the two strains of virus will decay at the same rate (since cytopathic effects and immune-mediated killing through other epitopes should occur at the same rate). Under these circumstances, even if we allow the immune response to be time dependent, the death rates for both strains will be the same at all times. Production and clearance rates of free WT and EM virus are given by p_W and p_M and by c_W and c_M, respectively.

We assume that all parameters, with the possible exception of δ, are constant in time. This not only implies a simple dynamic of target cells, infected cells, and virus but also neglects the possibility of the properties of WT and EM virus populations changing in time due to compensatory mutations. In this model, we have also neglected the point mutations of EM into WT and vice versa during the course of infection.

Since the turnover of virions is generally faster than the turnover of infected cells ($c_i \gg \delta_i$, where $i = W,M$), the number of infected cells closely follows the viral load, $I_W = (c_W/p_W)W$ and $I_M = (c_M/p_M)M$, so that the instantaneous rates of exponential growth g_W and g_M of the WT and EM virus can be, to a good approximation (31), written as

$$g_W = \frac{d \ln W}{dt} = \frac{1}{W}\frac{dW}{dt} = k_W \frac{p_W}{c_W} T - \delta(t) \equiv r_W T(t) - \delta(t) \tag{2}$$

$$g_M = \frac{d \ln M}{dt} = \frac{1}{M}\frac{dM}{dt} = k_M \frac{p_M}{c_M} T - \delta(t) \equiv r_M T(t) - \delta(t),$$

where $r_W = k_W p_W / c_W$ and $r_M = k_M p_M / c_M$ are the replicative capacities of the WT and EM virus, respectively. Replicative capacity is a compound effect of virus infectivity, production, and clearance, while target cells represent the most important feature of their shared environment. Positive values of g_W and g_M, when replication exceeds death, imply an increase in the viral load of each type, while negative values imply decay.

We define the instantaneous reversion rate, $R(t)$, at a given time, t, as the difference between the growth rates of WT and EM virus

$$R(t) = g_W - g_M \equiv (r_W - r_M) T(t) \tag{3}$$

where $r_W - r_M$ is the absolute fitness cost of the escape mutation or the absolute selection advantage of WT virus.

The relative growth of each type of virus depends not only on the different fitness of different virus types but also on the environment, most importantly on the target cell availability. When target cells are abundant, both types of virus will grow fast, and the differences in replicative capacity will in short time result in large differences in the viral load of each type. When target cells are scarce, the same differences in replicative capacity will result in a much slower change in the viral load ratio. Thus, the fitness cost of escape mutation may vary over time. We define the basic fitness cost as the fitness cost at a normal target cell number (i.e., soon after infection, before a significant number of $CD4^+$ T cells is infected or lost). The effective fitness cost is the fitness cost experienced at any point in time, dependent on the number of target cells available.

Similar reasoning was used previously (4, 26) to determine the relative fitness cost from in vitro reversion experiments. However, instead of the target cell

number, the authors used an unknown function of time to characterize the environment shared by WT and EM virus.

Since the escape mutation carries a fitness cost, $r_W > r_M$, the reversion rate in this simple model is always positive, meaning that WT virus will always outgrow EM virus if they are both present at the start of infection, when there is a large amount of available target cells and no immune response. The higher replicative fitness of WT will result either in faster growth or in slower decay.

Measuring the reversion rate from experimental data. The experimental data typically contain viral loads for wild-type (W) and EM (M) virus at different time points. The growth rates of the WT and EM, g_W and g_M, cannot then be found at each time point as in equation 2 but are defined between end points of a time interval. If viral loads are measured at time points t_s and t_e, the growth rates of WT g_W and EM g_M in a time interval starting at t_s and ending at t_e are determined from the experimental data, as follows

$$g_W(t_s, t_e) = \frac{\ln [W(t_e)/W(t_s)]}{t_e - t_s} \quad (4)$$

$$g_M(t_s, t_e) = \frac{\ln [M(t_e)/M(t_s)]}{t_e - t_s}$$

The growth rate is the average rate of exponential growth between the end points of the time interval. Negative growth rate implies decay.

The reversion rate, R, is again defined between end points of an interval, instead of at a single time point as in equation 3. In the time interval between t_s and t_e, the reversion rate is defined (11) as the difference between the growth rates of equation 4 of the WT and EM virus in the same interval

$$R(t_s, t_e) = g_W(t_s, t_e) - g_M(t_s, t_e) \quad (5)$$

which can be equivalently expressed in terms of the relative frequencies, $z(t) = W(t)/M(t)$, or in terms of WT and EM fractions, $f_W(t) = W(t)/[W(t) + M(t)]$ and $f_M(t) = M(t)/[W(t) + M(t)]$

$$R(t_s, t_e) = \frac{\ln [z(t_e)/z(t_s)]}{t_e - t_s} = \frac{\ln [f_W(t_e)/f_M(t_e)] - \ln [f_W(t_s)/f_M(t_s)]}{t_e - t_s} \quad (6)$$

This rate represents the estimate of the absolute difference between the replication rates of the two virus strains, with different sequences at the chosen epitope.

Measured reversion rate and target cell count in experimental data. If WT and EM virus differ only in one epitope and there are no mutations during the course of infection, then from equation 3, we expect the reversion rate to be proportional to the target cell number at each time point. However, both target cell numbers and viral loads are measured at discrete time points, and the reversion rate can be found experimentally only between end points t_s and t_e of a time interval, as in equation 5. So, what is the relationship between equation 5 and equation 3? We observe that the experimental reversion rate equation 5 between t_s and t_e can be written as the integral of the difference of instantaneous growth rates, so that

$$R(t_s, t_e) = \frac{1}{t_e - t_s}\int_{t_s}^{t_e} \frac{d}{dt}(\ln W - \ln M)dt = \frac{r_W - r_M}{t_e - t_s}\int_{t_s}^{t_e} T(t)dt = (r_W - r_M)T(t_s, t_e) \quad (7)$$

meaning that the reversion rate equation 5 between t_s and t_e will be proportional to the average number of target cells, $T(t_s, t_e)$, in this interval. Since the target cells are usually measured only at the end points, one needs to choose how to interpolate their number between the end points in order to evaluate the area under the curve on the right hand side of equation 7. If linear interpolation is chosen, the reversion rate, $R(t_s, t_e)$, will correspond to $T(t_s, t_e) = [T(t_s) + T(t_e)]/2$. If we assume exponential growth/decay, it will correspond to

$$T(t_s, t_e) = \frac{T_e - T_s}{\ln [T(t_e)/T(t_s)]} \quad (8)$$

Although neither interpolation method is entirely justified, we chose the exponential method defined by equation 8.

A simple model of escape. In escape, the mutant has the same replicative disadvantage as in reversion, but while the specific WT epitope is recognized by the CTLs, EM escapes CTL recognition at this epitope. The net effect of increased CTL killing of the WT virus is that the mutant with lower replicative capacity appears fitter in this environment and gets the sufficient selective advantage to overtake the wild type.

In the simple model of WT and EM dynamics equation 1, escape occurs when the death rate of WT-infected cells, δ_W, becomes higher than the death rate of EM-infected cells, δ_M, because of WT-specific CTL killing, so that the escape rate

$$E(t) = g_M - g_W = \delta_W(t) - \delta_M(t) - (r_W - r_M)T(t) \quad (9)$$

becomes positive. This happens when the damaging results of increased killing of WT-infected cells overcome its replicative advantage. The difference between WT-infected and EM-infected cell death rates is not related to target cell numbers, but we expect it to increase with $CD8^+$ numbers associated with the escape epitope. The effects of the replicative advantage will be, on the other hand, more beneficial for WT virus when there are more target cells available.

If we assume that the WT-infected and EM-infected cell death rates are different ($\delta_W > \delta_M$) but do not change in time, then escape is faster at low numbers of targets (usually in the viral load decay phase). In contrast, the ability of the EM virus to establish infection depends on its ability to grow at the time of its appearance ($g_M = r_M T - \delta_M$ must be positive), which is larger for a larger target pool. Therefore, for a constant difference in death rates, the escape rate is the lowest where the EM growth rate is the highest.

In reality, the time dependence of the escape rate is due to both the target cell limitation and the WT-specific immune response changing in time. This is why EM does not have to have an advantage at all times.

In the expression for escape rate equation 9, the last term on the right-hand side actually represents the reversion that would occur if there were no specific CTL killing of WT-infected cells. If we know the difference between the replicative capacities of the WT and the EM, $r_W - r_M$, from reversion experiments with the same virus and can measure the observed escape rate, E, we can estimate the time-dependent WT killing rate, K, from

$$K(t) = \delta_W(t) - \delta_M(t) = E(t) + (r_W - r_M)T(t) \quad (10)$$

Estimating escape rate from experimental data. The escape rate, E (or the replacement rate of the WT by the EM), between time points t_s and t_e is calculated from the difference between the growth rates (equation 4) of the EM and WT

$$E(t_s, t_e) = g_M(t_s, t_e) - g_W(t_s, t_e) = -\frac{\ln [z(t_e)/z(t_s)]}{t_e - t_s} \quad (11)$$

where $z(t) = W(t)/M(t)$.

From the experimental data, we can determine only the escape rate in a given time interval, so that the killing rate in the time interval (t_s, t_e) is

$$K(t_s, t_e) = E(t_s, t_e) + (r_W - r_M)T(t_s, t_e) \quad (12)$$

where $T(t_s, t_e)$ is the average number of target cells in the interval.

RESULTS

The $CD4^+$ T-cell number determines the reversion rate. It has been conjectured that the reversion rate should follow general virus growth trends (18). However, we have found that the correlation between the total viral load growth rate and the reversion rate is weak (24). We hypothesized that a more important driver of the reversion of EM virus would be the viruses' ability to grow and replicate efficiently when they expand exponentially in large numbers of available target cells. Analysis of the basic model of viral dynamics suggests that the rate at which reversion occurs should be directly proportional to the number of uninfected target cells (equation 3). Therefore, we compared the rate of reversion at different time intervals to the total $CD4^+$ T-cell count in peripheral blood. Since $SHIV_{mn229}$ is a CXCR4-tropic virus and can thus infect both naïve and memory $CD4^+$ T cells, it was not necessary to consider the different potential subsets of $CD4^+$ T cells. Using experimental data for the viral loads of WT and EM virus over time, measured using quantitative real-time PCR, we estimated the reversion rates over time in macaques, following

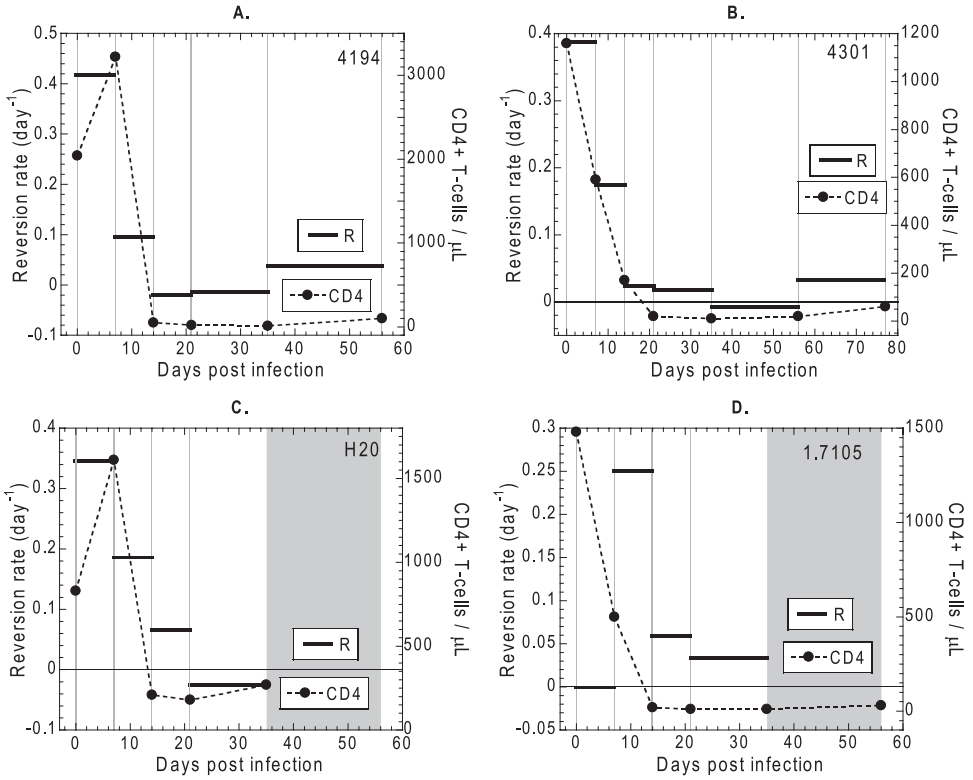

FIG. 1. Relationship between $CD4^+$ T-cell numbers and reversion rate. For each animal, the number of $CD4^+$ T cells (right-side axis) is plotted against the estimated rate of reversion (left-side axis) during each time interval. The reversion rate and $CD4^+$ T-cell number appear closely linked over time, with the exception of the first time interval for animal 1.7105, where no reversion is observed in the first time period (circles). Gray areas indicate time periods where reversion was unable to be calculated.

infection with $SHIV_{mn229}$. The $SHIV_{mn229}$ challenge stock used has been shown to be ~10% WT and ~90% EM virus at the KP9 epitope, and thus, both viral variants were present at the time of infection. The calculated reversion rates and the $CD4^+$ T-cell numbers over frequent time intervals during acute and postacute SHIV infection for the four animals are shown in Fig. 1A to D. There was a close temporal relationship between reversion rates and $CD4^+$ T-cell levels.

If we plot the reversion rate against the average number of target $CD4^+$ T-cells (estimated using equation 8) in each interval, we find a strong correlation (Fig. 2A), albeit with a different slope for each animal. However, the normal number of $CD4^+$ T cells in blood is quite variable among healthy animals (and humans) and may simply reflect the proportion of the total body $CD4^+$ T-cell pool in the blood of that animal, whereas the total body pool may be more consistent between animals. In order to overcome this, instead of considering the absolute number of $CD4^+$ T cells in the animal's blood, we may consider the relative number of $CD4^+$ T cells at any time compared to the baseline number for that animal. If we normalize the number of targets at any time by the average number during the first week, we see that there is a strong relationship between the reversion rate and the relative target cell number in the different animals ($r^2 = 0.552$; $P = 0.0003$) (Fig. 2B).

The slope of this line is a measure of how the observed reversion rate varies with target cell number. We interpret this result as implying that the different slopes in Fig. 3A do not reflect different replicative capacities of WT and EM virus in different animals but that they reflect different percentages of the (generally quite similar) total body $CD4^+$ numbers found in blood of different animals.

In one animal (Fig. 1D, 1.7105), reversion did not follow the general pattern predicted by equation 3. In this animal, there was no reversion during the first week of infection, but later on, the reversion rate followed the trend of CD4 numbers. This 1-week delay in reversion cannot be explained within the framework of our simple model but may require a more complex description with, for example, explicit delays and separate treatment of latently infected cells. The point corresponding to the initial zero reversion rate in this animal is shown in Fig. 2 (gray circles).

Predicting periods when new mutants are unable to grow. The observation that reduced target cell numbers lead to reduced effective fitness cost later in infection implies that reversion in vivo for the same epitope will occur with various rates during the course of infection. In the cases we have studied here, animals were infected with a mixture of WT and EM virus, and thus, there was no requirement for the virus to mutate to generate the competing quasi-species. However, in many HIV-1 transmission settings, a clonal population of WT or EM virus will be transmitted (13), and the competing virus must first be generated through mutation, then survive the early period of growth, and then compete to become dominant

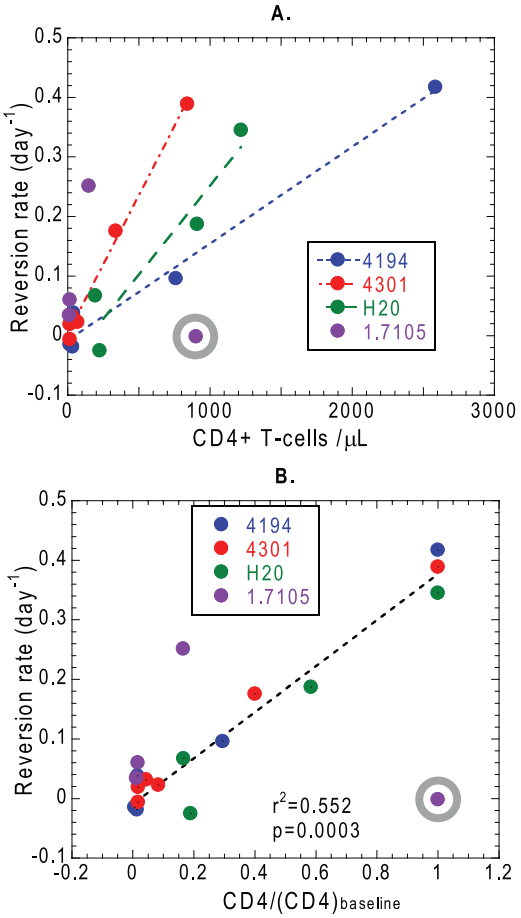

FIG. 2. Reversion rate is strongly correlated with $CD4^+$ T-cell number. (A) The calculated reversion rate and absolute $CD4^+$ T-cell number are plotted for each animal. (B) The number of $CD4^+$ T cells is normalized to the baseline level for each animal. There is a significant correlation between normalized CD4 levels and reversion rates (values for Spearman's test are indicated). For the purposes of calculating effective fitness cost used later in the study, the linear relationship (dashed line) between normalized CD4 level and reversion rate was estimated, excluding the data for animal 1.7105 (for this line, $r^2 = 0.97$; $P < 0.0001$).

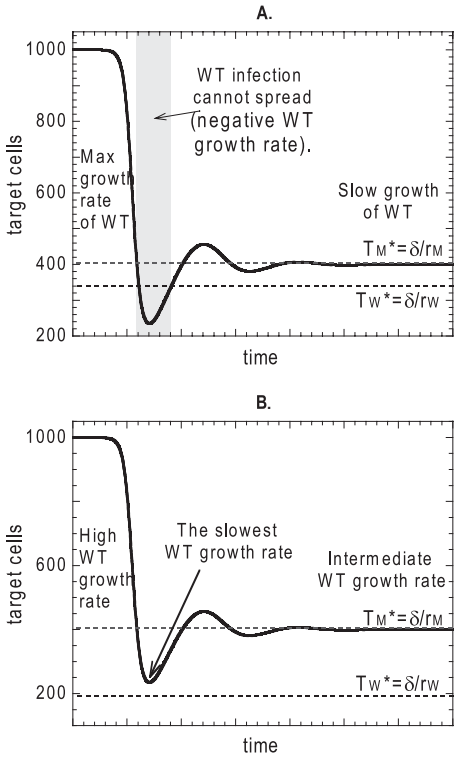

FIG. 3. Conditions for growth of the WT virus if it appears by mutation later in the EM infection. When a viral strain arises de novo by mutation, it must have an initial growth rate greater than zero in order to spread. During the nadir in target cell numbers in acute infection, it is possible that the WT virus will be unable to propagate because of extremely low target cell levels (gray area) if there is a low basic fitness cost of the EM virus (A). At high basic fitness cost of EM virus the WT virus will always have a positive growth rate (B). The same arguments apply to the spread of the EM virus in WT infection.

in vivo. This process will often lead to a significant delay before the WT-revertant virus is detected, and depending on when this occurs, we predict different dynamics will be observed. Where the WT virus is present early in infection, it will benefit from a high effective fitness cost of escape mutation and be rapidly selected. However, where WT virus is first generated around the peak of infection (the nadir of target cells during acute infection), either it may compete poorly with EM virus (which has a low effective fitness cost at low target cell numbers) or it may even be lost if target cells at the nadir are already severely depleted by the mutant virus. In chronic infection, low target cell numbers will lead to a slow reversion to the WT virus.

This response can be better understood from Fig. 3, in which the variation in target cell numbers during the infection by EM virus is shown. In the steady state, when the EM virus is neither growing nor decaying ($g_M = 0$, in equation 2), the target cell number will be at the equilibrium level, at $T^*_M = \delta/r_M$. For target cell numbers higher than the T^*_M value, the EM virus will grow, and for target cell numbers lower than the T^*_M value, it will decay (equation 2). The target cell number that would lead to the set point (equilibrium level) in WT virus infection is always lower than the equilibrium target cell level in EM infection (because the WT has a higher replication rate); thus, $T^*_M = \delta/r_W < T^*_M$. If the WT appears by mutation during the EM infection when T is more than T^*_M (i.e., the target cell number is greater than the equilibrium level for the WT virus, which occurs with early infection or in chronic infection), the WT virus will be able to grow and eventually outgrow the EM virus. Around the nadir of target cells, when the number of target cells is less than the equilibrium value for the WT virus ($T < T^*_M$; Fig. 3A), the basic reproductive ratio for the WT virus will be <1, and if the WT virus initially arises here, it will likely be lost.

Thus, depending on the timing of when the WT virus arises, it has a higher or lower probability of survival. If it arises early and expands sufficiently during the period of high target cell availability, then it will not be lost during the contraction phase of virus and will still slowly overtake the EM virus but at a very low rate. If it just appeared by mutation at such low target cell numbers, it would disappear because it would not be able to grow. The possibility of growth of the WT virus around the target cell nadir in the EM infection depends on the cost of the

TABLE 1. Basic fitness cost overestimates killing rate[a]

Animal	Maximum escape rate (E_{max}/day)	CTL killing rate estimated plus basic fitness cost (R_{max} + E_{max}/day)	CTL killing rate estimated using effective fitness cost ($E = E_{max}$/day)
6276	0.514	0.898	0.606
5614	0.409	0.793	0.570
5712	0.252	0.636	0.253
6167	0.046	0.430	0.054

[a] The maximum escape rate was estimated for four animals infected with $SHIV_{mn229}$. The CTL killing rate through the KP9 epitope was then calculated in two ways. First, we estimated the killing rate as previously described, using the maximum reversion rate observed (the basic fitness cost). CTL killing was substantially lower when it was estimated by using the effective fitness cost calculated from the number of $CD4^+$ T-cell targets at the time of escape.

escape mutation. If the cost is high and the replicative capacity of the EM is much impaired ($r_M \ll r_W$), then target cells will not be sufficiently depleted, even at the nadir, and the WT infection will always be able to spread (Fig. 3B). The windows where the WT cannot appear despite its replicative advantage exist only if the cost of escape mutation is not too high.

Similar arguments apply to the propagation and survival of the EM during WT infection in escape, but here the situation is more complex because the amount of depletion at the nadir of target cells in WT infection depends on the effectiveness of CTL killing at this time point.

Estimating the killing rate from the escape rate. The observed rate of immune escape is the balance of the immune advantage of the EM virus avoiding CTL recognition versus the fitness costs of escape. The immune advantage in this case is the reduced CTL killing rate of the EM virus. Thus, the CTL killing rate can be inferred as the sum of the observed escape rate and the fitness cost. We previously estimated the killing rate at the KP9 epitope to be 1.31 day^{-1} during acute infection (11). However, this estimate included the basic fitness cost (maximal reversion rate estimated during the first week, 0.38 day^{-1}) and the maximal escape rate (estimated during the third and fourth week). Since the effective reversion rate is substantially lower during the third and fourth week, using the basic reversion rate estimated in the first week will tend to overestimate the killing rate (16). Understanding the relationship between the target cell number and the reversion rate described above allows us to estimate the effective fitness cost at any time from data for the number of target cells, using equation 12. We determined the difference in replicative capacities from the slope of the line in Fig. 2B [$(r_W - r_M)\, T_{baseline} = 0.387 \pm 0.02$ day^{-1}], obtained by linear regression without taking into account the anomalous data points belonging to animal 1.7105 (for this line, $r^2 = 0.97$; $P < 0.0001$).

In order to examine the relationship between virus escape and epitope-specific $CD8^+$ T cells, we followed the escape rates and KP9-specific CTL levels in four responder (*Mane-A*10*-positive) macaques infected with $SHIV_{mn229}$, which demonstrated an early reversion to the WT, followed by reescape (described in references 10 and 24). Table 1 illustrates the differences in killing rates estimated by using the basic fitness cost value versus the effective fitness cost value. The mean basic fitness cost estimated from the maximal reversion rate in the first week is 0.38 day^{-1}. Using this estimate of fitness cost (and adding it to the escape rate), we would estimate the killing rates at between 0.43 day^{-1} and 0.90 day^{-1} (equivalent to the half-lives for killing through the KP9 epitope of approximately 18 to 39 h). However, since the maximal escape rate occurred later in infection, the effective fitness costs at this time were significantly lower. Incorporating the effective fitness costs into the killing rate calculation leads to significantly lower estimates of the killing rate, from 0.05 day^{-1} to 0.61 day^{-1} (equivalent to the half-lives for killing through KP9 of between approximately 27 h and 13 days) (Table 1). In fact, escape and killing rates differ significantly only when there is not much $CD4^+$ depletion (Fig. 4A). In addition, the timing of maximal killing rate can also change once the effective fitness cost is considered. That is, since the maximal effective fitness cost, *R*, does not coincide with the highest escape rate, *E* (Fig. 4A), so maximal CTL killing may not occur at the maximum of observed escape rate (Fig. 4B). For animal 6276, the maximal escape rate is between days 10 and 13, and thus, when the basic fitness cost is considered, the maximal killing rate occurs at the same time. When the effective fitness cost is added, the maximal killing rate is found to be between days 7 and 10.

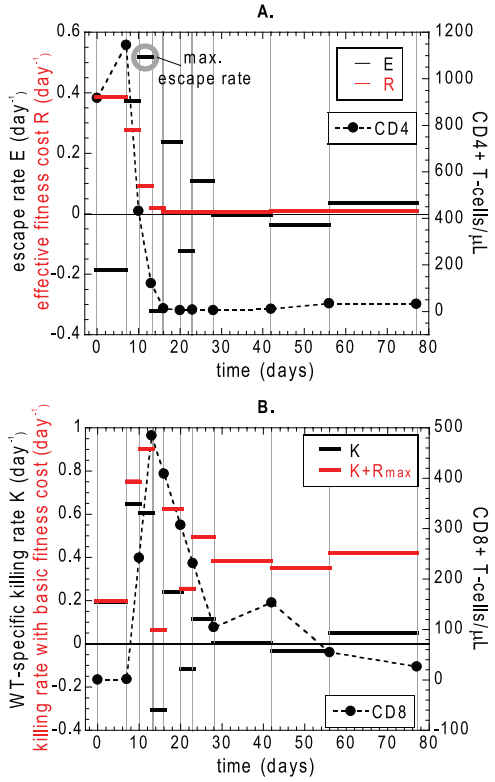

FIG. 4. Estimating the killing rate using the effective fitness cost. (A) The measured escape rate (black) and estimated effective fitness cost (red, estimated from the relationship described in the legend to Fig. 2B) are shown for animal 6276. The estimated killing rate is the sum of the escape rate and effective fitness cost. In late escape, the effective fitness cost is almost negligible. (B) The WT-specific killing rate estimated using an earlier approach (red, determined using the basic fitness cost, as in reference 11) tends to overestimate the actual killing rate. The actual WT-specific killing rate (black bars) estimated using the effective fitness cost is substantially lower at all times after the first time interval. The maximal escape rate does not necessarily coincide with the maximum killing rate.

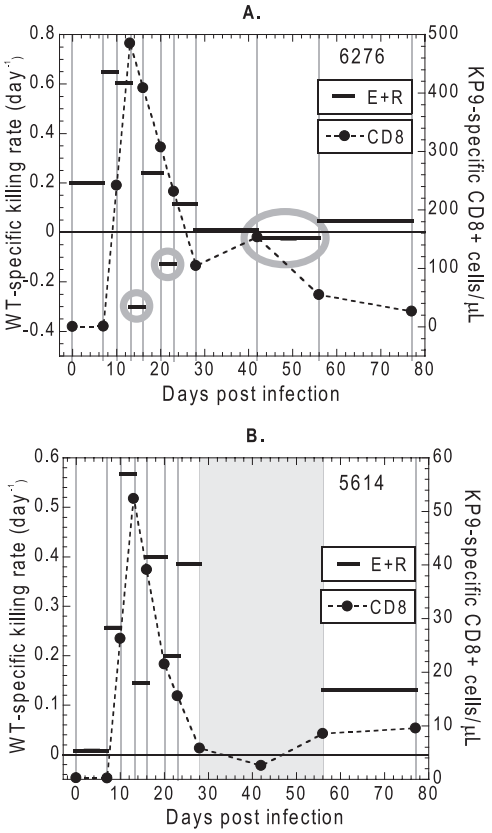

FIG. 5. Rapid fluctuations in the killing rate around the peak of CTL. Although the estimated killing rate generally follows the magnitude of the $CD8^+$ T-cell response, there are major fluctuations from the highest to the very lowest observed killing rate around the peak of the $CD8^+$ T-cell response in animals 6276 and 5614. Animal 6276 even has negative killing rates in three time intervals (circled in gray). This suggests a more complicated dynamic of immune control than would be predicted by a straight "CD8-killing" model.

Killing rate correlates poorly with the specific $CD8^+$ T-cell number. Once the killing rate can be accurately estimated from data for EM and WT viral loads and $CD4^+$ T-cell count, it is expected that this should be directly correlated with the magnitude of the $CD8^+$ T-cell response to the epitope. In Fig. 5, we show a time course for the killing rate and the KP9-specific $CD8^+$ numbers for two vaccinated animals, 6276, vaccinated with the DNA/FPV vaccine (Fig. 5A), and 5614, vaccinated with DNA only (Fig. 5B). The killing rate generally follows the trend of $CD8^+$ numbers in both animals. The DNA/FPV vaccine (animal 6276) appears at first sight to be more efficient than the DNA-only vaccine (animal 5614), since it generates approximately 10-fold larger epitope-specific CTL levels at all times. However, if we compare the killing rates, we see that they are quite similar, implying that the CTL number is not always indicative of their efficiency.

When we plotted the WT-specific killing rates for all four *Mane-A*10*$^+$ animals against the number of KP9-specific $CD8^+$ T cells present at that time (measured using MHC class I peptide tetramers), we found that there was no significant correlation, as shown in Fig. 6A. The poor correlation (Spearman's $r = 0.1395$; $P = 0.403$) is mostly due to the three points with negative killing rates (i.e., reversion to the WT) at elevated CTL levels (Fig. 5A and 6A, circled in gray), belonging to animal 6276. These points correspond to surprisingly large fluctuations from the highest killing rate to the very lowest (or even negative) killing rates observed also with control animals 6167 and 5712. (The negative killing rate value would mean an advantage of the WT larger than expected from its fitness advantage without any CTL killing.)

It is not clear if the large fluctuations in killing rate and the lack of significant correlations between CTL killing and CTL numbers are consequences of statistical errors in the determination of WT and EM viral loads at different time points or if they reflect some unexplained effect of CTL control not taken into account in our model (e.g., latently infected cells, the role of $CD4^+$ T-cell help [25] for the activation of killing functionality of CTLs, or noncytolytic CTL function).

The large fluctuations are often seen around the peaks of both viral load and CTL numbers. Although such fluctuations appear unusual, similar fluctuations and negative escape rates closely following the periods of the fastest outgrowth of the mutant were also found in four out of the eight animals described in a recent paper in which the role of $CD4^+$ T-cell help in CTL killing in SIV viral escape was estimated (25). In that study, the authors assumed the direct proportionality between the killing rate, K, and the CTL numbers, E_W [$K(t) = \kappa E_W(t)$], and found the best fit for the killing constant, κ, from the time dependence of the EM fraction in time. The periods of negative escape rates were smoothed out in this process. We did not make any assumptions about the form of dependence between CTL numbers and killing rate and avoided data manipulation such as smoothing in order not to mask any real effects.

Surprisingly, we found a significant correlation between the $CD4^+$ T-cell numbers from all four animals and killing rates (Fig. 6C, Spearman's $P = 0.0008$). Although the correlations were not significant from the smaller number of data points in each individual animal, the correlation values were consistently stronger for the $CD4^+$ T-cell numbers and the WT-killing rate than for the correlation between the number of tetramer-positive cells and the WT-killing rate. The positive correlation between target cell numbers and killing rate supports the hypothesis of the need for $CD4^+$ help in CTL killing (25). It is also consistent with some noncytolytic CTL function. The effect of noncytolytic control of infection (either by KP9-specific or other CTL) would be to reduce the effective fitness cost by decreasing the overall replication of the virus and would therefore be proportional to the target cell numbers in addition to the dependence on CTL levels.

DISCUSSION

Identifying HIV vaccine targets based upon the rate of escape or inferred fitness cost of these epitopes is a step toward the rational design of better T-cell vaccines (11, 14, 20). In addition, a comparison of escape rates and fitness costs has been performed between HIV and SHIV/SIV infection (3) and between epitopes in the same infection (14, 23) to understand immune control of virus. A major difficulty with previous studies is that these comparisons are often performed at different stages of infection and may therefore be confounded by the different dynamics of infection (24). In vitro studies have pre-

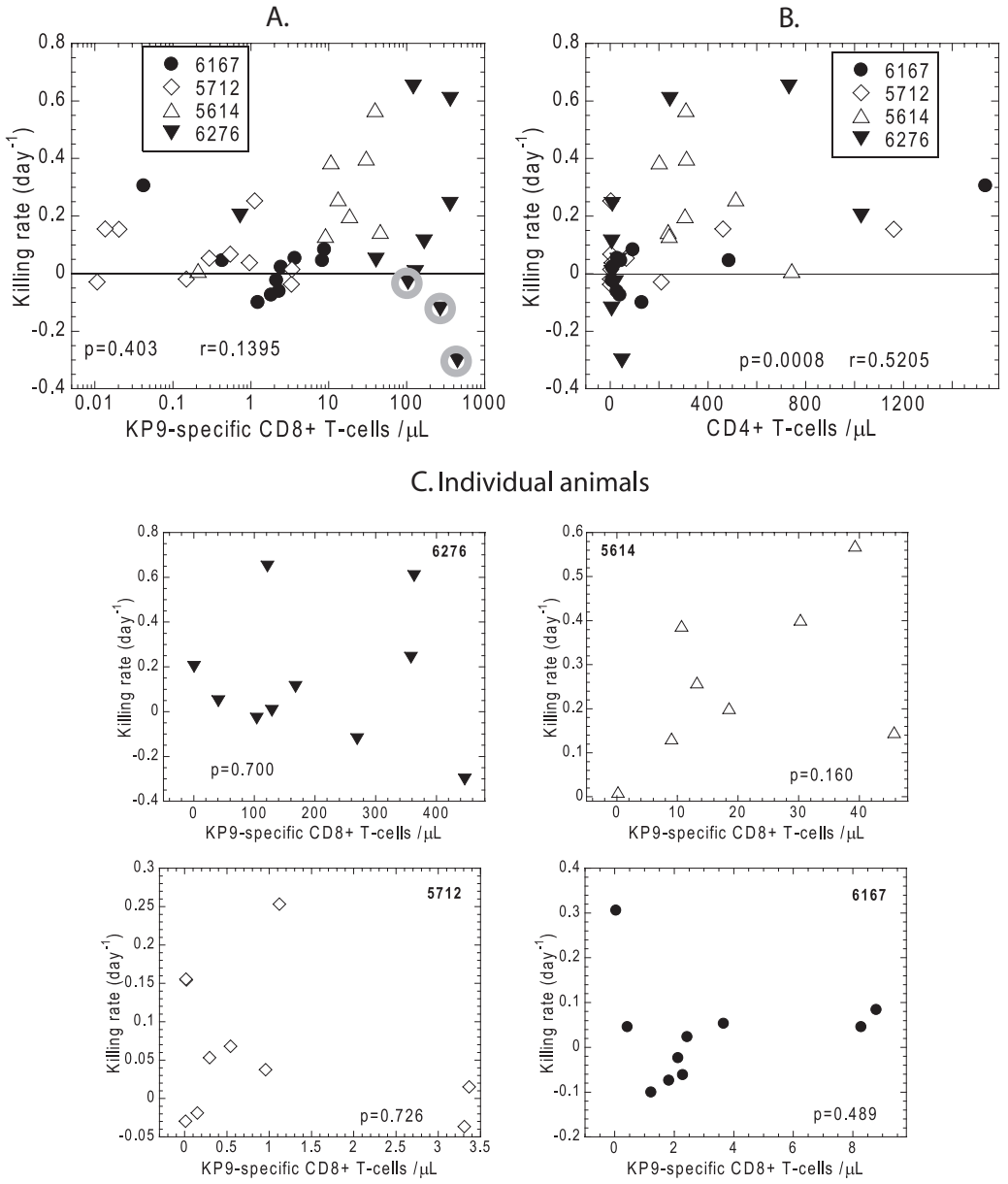

FIG. 6. Poor correlation between KP9-specific $CD8^+$ T-cell numbers and the killing rate. The number of KP9-specific $CD8^+$ T cells (detected using MHC class I peptide tetramers) is relatively poorly correlated with the estimated killing rate in individual animals.

viously suggested that target cell availability may play a role in the viral competition between drug-resistant and wild-type viruses (35). Here we demonstrate that a basic viral dynamics model predicts a relationship between the rate of reversion of escape mutation and the number of target $CD4^+$ T cells available for infection and that this relationship is observed for experimental studies of reversion in vivo for the CXCR4-tropic SHIV infection of pigtail macaques, where target cells can be easily identified and measured. Importantly, the maximal reversion rate estimated very early in infection gives an estimate of the basic fitness cost (the fitness cost in the presence of normal target cell numbers), but the effective fitness cost (fitness cost at a given time or number of target cells) is often much lower than this. Thus, depending on when the WT virus arises, it may revert rapidly, die out early, or revert slowly (Fig. 7A).

Similarly, the rate of immune escape will be significantly affected by the timing of generation of the EM virus. Figure 7B shows what we would expect if the preferential CTL killing of the WT-infected target cells were constant in time (δ_W and δ_M in equation 9 are constants). Immediately after infection, the EM virus pays the highest effective fitness cost, and thus, the EM virus will be selected during this time only if it has extremely low fitness costs or if there is extremely high CTL killing. By contrast, the fastest escape will be observed when target cells are depleted following the peak of viremia. At this time, even EM viruses with extremely high fitness costs may be selected. In chronic infection, effective fitness costs are still

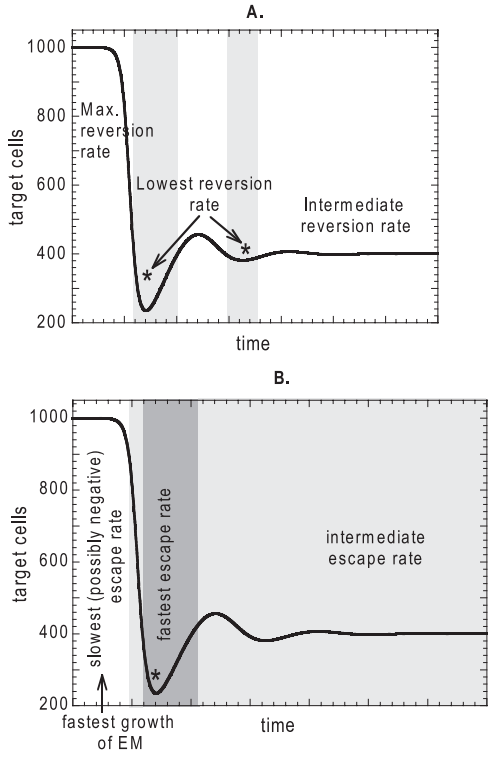

FIG. 7. Target cell availability determines escape and reversion kinetics (schematic). (A) The expected rate of reversion varies during infection with the number of target cells. The highest reversion is seen immediately after infection, where the basic fitness cost is observed. However, following the peak of virus, extremely slow reversion is seen during the nadir of target cells due to low effective fitness cost. The WT virus arising during this period may die out due to stochastic effects because its growth rate is negative (asterisk). (B) Varying the effective fitness cost leads to slow viral escape immediately after infection (white field), where the mutants can grow faster than the WT only if they have very low fitness cost or if there is extremely high CTL killing of the WT. This is followed by a period of extremely low effective fitness cost just after the peak of virus, where even extremely unfit or weakly killed viruses may be selected if they are already present. However, if the mutants appear during this period, they may disappear due to stochastic effects (dark gray field marked with an asterisk). In chronic infection (light gray area) there is an intermediate effective fitness cost where mutant viruses will escape slowly.

relatively low, so viruses with high fitness costs or low CTL killing can be selected. Importantly, the early dynamics are extremely fast, and definitions of acute infection may span periods of extremely high, low, or intermediate effective fitness cost, and care must be taken when comparing these periods.

It should be stressed at this point that our model (expressed in equation 1 and Fig. 7) represents an idealized picture of reversion and escape, with approximations regarding both the virus populations and target cell numbers. In the model, we assume that the WT and EM virus populations differ only at one epitope and do not experience compensatory mutations that might change their fitness over the course of infection. However, the real-time PCR assay used in the experimental studies measures all virus particles with the WT sequence at the KP9 epitope. Similarly, measurements of the EM virus represent all virus particles with the EM sequence at the same epitope. Thus, this approach would not detect compensatory mutations or escape at other epitopes that may evolve over the course of infection. We note that in our previous studies using direct sequencing of the viral Gag gene (10, 11), we have sequenced many hundreds of WT and EM viruses on multiple occasions and have not detected any clear patterns of compensatory or other mutations that might affect selection. Thus, it seems unlikely that compensatory mutations are playing a large role in affecting viral fitness in this study.

With respect to the target cells, the model implicitly assumes that all target cells can be infected with equal probability by each strain of virus (i.e., WT or EM) and would produce the same amount of virus when infected. However, the replicative capacity of virus is thought to differ between naïve and memory CD4 T cells and according to the activation state of the cell (39). Moreover, the number and activation state of targets in different subsets may change in time, affecting the replicative capacity of virus (33). Thus, although we assume that the $CD4^+$ T-cell measurements in peripheral blood always reflect the availability of target cells, both the location of target cells in different anatomical locations, their phenotypes, and the activation state of these cells may differ with time. In our study, we observed a linear relationship between the target cell levels and the reversion rate, suggesting that the effects of compensatory mutations and variations in subsets of $CD4^+$ T cells and their distributions in anatomical compartments were negligible, so that reversion rate was nearly "ideal."

Although our study was limited to an X4-tropic SHIV, we expect much of the analysis regarding the target cell dependence of reversion and escape rates is applicable to R5-tropic SIV and HIV infections under the idealized conditions considered in the model. However, in CCR5-tropic virus infections such as those caused by HIV and SIV, estimating the effective fitness costs may be more difficult, since the precise phenotype, anatomical location, and activation state of target cells are not well defined and may change over the course of infection (30). Consequently, it may be difficult to unambiguously define the target cells in R5-tropic infections, although we expect that the relationships between target cell numbers and growth rates would still apply. The reversion rate would still reflect the underlying target cell numbers, while the escape rate would still be given by the general expression as the balance of fitness cost and the difference in death rates of infected cells. On the other hand, the combination of the varying composition of target cell pool and its varying distribution over the anatomical compartments, as well as changes in composition of WT and EM populations, may have a much stronger impact in HIV infection.

The differences in target pool phenotype and turnover between X4-tropic SHIV and R5-tropic SIV or HIV may result in target cell numbers following a different time dependence in these infections compared to that shown in Fig. 7. However, when a defined population of target cells in the gut was studied (37), the dynamics of target cell depletion appeared to be similar to that observed for CXCR4 virus infection (7), suggesting that the dynamics of target cells may be similar when they can be measured directly. Specifically, memory $CD4^+$ T-cells, considered the main targets of HIV, are severely depleted in the chronic infection phase. Thus, the near absence of reversion to the WT virus in chronic, progressive HIV infection, when the immune pressure due to CTL activity is much

decreased, can be explained by relatively small target cell pool at this stage of infection.

The $CD8^+$ T-cell response to HIV infection is stimulated by the presence of virus and can vary greatly with time. In addition, not all $CD8^+$ T-cell responses arise simultaneously: some responses peak early in infection (around the peak of viral load), while others may develop slowly in chronic infection (38). For CTL responses that are the highest around the peak in viral load (and nadir of $CD4^+$ T cells during acute infection), maximal killing will coincide with minimal effective fitness cost and lead to extremely rapid selection of EM virus at this time. However, for responses that peak later in infection, the peak in killing may coincide with an intermediate effective fitness cost, slowing viral escape. Importantly, vaccination is likely to have the effect of bringing forward the peak in $CD8^+$ T-cell response; in some cases, it may bring the peak in WT killing forward in time to coincide with the nadir in effective fitness cost and lead to rapid escape at an epitope which would otherwise experience slow escape and more prolonged immune pressure. This hypothesis is testable with future studies of larger numbers of macaques or human subjects in randomized vaccine trials, for example in the recently stopped adenovirus-recombinant HIV vaccine trial (29). Analyses of the fine kinetics of T-cell escape and viral loads in subjects that become infected despite vaccination could identify useful HIV antigens for future HIV vaccine studies.

Since it is rare for the EM and WT viral loads to be estimated around the peak of viral load in HIV infection, it is not surprising that the estimated rate of immune escape in HIV is lower than in SHIV/SIV, where the maximal escape rate is usually measured just after the peak of viral load (3). Even when analyses are limited to acute infection, this definition for HIV can be extremely broad (i.e., up to 6 months). Similarly, an association between an increased number of escape mutations and a lower $CD4^+$ T-cell count suggests that increased escape is associated with disease progression (5). However, this analysis may be confounded by the fact that lower $CD4^+$ T-cell levels may lead to lower effective fitness cost, and thus, permit the selection of EM virus at epitopes with higher fitness cost or lower killing. Comparison of the frequency of escape mutations in responders (bearing the correct MHC) versus nonresponders has been another means of estimating the rate of escape and reversion (12, 28). However, these frequencies are inevitably linked to not only the rate of selection, but also the timing of mutation (if the mutant is not present in the inoculum). Thus, a WT virus that arises early (i.e., is easily produced by mutation) will be rapidly selected and dominate from early infection. However, a WT virus that evolves only later around the peak of infection may initially be lost due to a minimal fitness cost of EM virus and a negative overall viral growth rate. A WT virus that arises even later will only be slowly selected and may be detected only for a shorter proportion of the period of infection (and thus, have a lower frequency in the MHC-negative population and appear to have a low fitness). Thus, the timing, rate, and frequency of reversion observed in vivo are governed both by the probability of mutation and by the effective fitness cost.

The dynamics of immune escape and reversion in vivo present a complex balance of CTL killing and effective fitness cost and determine both the viral quasispecies within the host and that circulating within the host population. Optimal targeting of the CTL response to epitopes with high fitness cost may be one mechanism to maximize vaccine effectiveness. Here, we demonstrate the important role played by $CD4^+$ target cells for infection in determining the dynamics of escape and reversion and suggest that this effect needs to be taken into account when viral dynamics in vivo are studied. Further studies should aim to verify this effect in HIV.

ACKNOWLEDGMENTS

We thank Ruy Ribeiro for review of the manuscript and helpful discussion.

This work was supported by the James S. McDonnell Foundation 21st Century Research Award/Studying Complex Systems and by the Australian National Health and Medical Research Council (NHMRC). M.P.D. is a Sylvia and Charles Viertel Senior Medical Research Fellow.

REFERENCES

1. **Allen, T. M., M. Altfeld, X. G. Yu, K. M. O'Sullivan, M. Lichterfeld, S. Le Gall, M. John, B. R. Mothe, P. K. Lee, E. T. Kalife, D. E. Cohen, K. A. Freedberg, D. A. Strick, M. N. Johnston, A. Sette, E. S. Rosenberg, S. A. Mallal, P. J. Goulder, C. Brander, and B. D. Walker.** 2004. Selection, transmission, and reversion of an antigen-processing cytotoxic T-lymphocyte escape mutation in human immunodeficiency virus type 1 infection. J. Virol. **78:**7069–7078.
2. **Allen, T. M., D. H. O'Connor, P. Jing, J. L. Dzuris, B. R. Mothe, T. U. Vogel, E. Dunphy, M. E. Liebl, C. Emerson, N. Wilson, K. J. Kunstman, X. Wang, D. B. Allison, A. L. Hughes, R. C. Desrosiers, J. D. Altman, S. M. Wolinsky, A. Sette, and D. I. Watkins.** 2000. Tat-specific cytotoxic T lymphocytes select for SIV escape variants during resolution of primary viraemia. Nature **407:** 386–390.
3. **Asquith, B., and A. R. McLean.** 2007. In vivo CD8+ T cell control of immunodeficiency virus infection in humans and macaques. Proc. Natl. Acad. Sci. USA **104:**6365–6370.
4. **Bonhoeffer, S., A. D. Barbour, and R. J. De Boer.** 2002. Procedures for reliable estimation of viral fitness from time-series data. Proc. R. Soc. Lond. B Biol. Sci. **269:**1887–1893.
5. **Brumme, Z. L., C. J. Brumme, D. Heckerman, B. T. Korber, M. Daniels, J. Carlson, C. Kadie, T. Bhattacharya, C. Chui, J. Szinger, T. Mo, R. S. Hogg, J. S. Montaner, N. Frahm, C. Brander, B. D. Walker, and P. R. Harrigan.** 2007. Evidence of differential HLA class I-mediated viral evolution in functional and accessory/regulatory genes of HIV-1. PLoS Pathog. **3:**e94.
6. **Dale, C. J., R. De Rose, I. Stratov, S. Chea, D. C. Montefiori, S. Thomson, I. A. Ramshaw, B. E. Coupar, D. B. Boyle, M. Law, and S. J. Kent.** 2004. Efficacy of DNA and fowlpox virus priming/boosting vaccines for simian/human immunodeficiency virus. J. Virol. **78:**13819–13828.
7. **Davenport, M. P., L. Zhang, J. W. Shiver, D. R. Casmiro, R. M. Ribeiro, and A. S. Perelson.** 2006. Influence of peak viral load on the extent of CD4+ T-cell depletion in simian HIV infection. J. Acquir. Immune Defic. Syndr. **41:**259–265.
8. **De Rose, R., C. J. Batten, M. Z. Smith, C. S. Fernandez, V. Peut, S. Thomson, I. A. Ramshaw, B. E. Coupar, D. B. Boyle, V. Venturi, M. P. Davenport, and S. J. Kent.** 2007. Comparative efficacy of subtype AE simian-human immunodeficiency virus priming and boosting vaccines in pigtail macaques. J. Virol. **81:**292–300.
9. **Evans, D. T., D. H. O'Connor, P. Jing, J. L. Dzuris, J. Sidney, J. da Silva, T. M. Allen, H. Horton, J. E. Venham, R. A. Rudersdorf, T. Vogel, C. D. Pauza, R. E. Bontrop, R. DeMars, A. Sette, A. L. Hughes, and D. I. Watkins.** 1999. Virus-specific cytotoxic T-lymphocyte responses select for amino-acid variation in simian immunodeficiency virus Env and Nef. Nat. Med. **5:**1270–1276.
10. **Fernandez, C. S., M. Z. Smith, C. J. Batten, R. De Rose, J. C. Reece, E. Rollman, V. Venturi, M. P. Davenport, and S. J. Kent.** 2007. Vaccine-induced T cells control reversion of AIDS virus immune escape mutants. J. Virol. **81:**4137–4144.
11. **Fernandez, C. S., I. Stratov, R. De Rose, K. Walsh, C. J. Dale, M. Z. Smith, M. B. Agy, S. L. Hu, K. Krebs, D. I. Watkins, H. O'Connor, D. M. P. Davenport, and S. J. Kent.** 2005. Rapid viral escape at an immunodominant simian-human immunodeficiency virus cytotoxic T-lymphocyte epitope exacts a dramatic fitness cost. J. Virol. **79:**5721–5731.
12. **Frater, A. J., H. Brown, A. Oxenius, H. F. Gunthard, B. Hirschel, N. Robinson, A. J. Leslie, R. Payne, H. Crawford, A. Prendergast, C. Brander, P. Kiepiela, B. D. Walker, P. J. Goulder, A. McLean, and R. E. Phillips.** 2007. Effective T-cell responses select human immunodeficiency virus mutants and slow disease progression. J. Virol. **81:**6742–6751.
13. **Frater, A. J., C. T. Edwards, N. McCarthy, J. Fox, H. Brown, A. Milicic, N.**

Mackie, T. Pillay, J. W. Drijfhout, S. Dustan, J. R. Clarke, E. C. Holmes, H. T. Zhang, K. Pfafferott, P. J. Goulder, M. O. McClure, J. Weber, R. E. Phillips, and S. Fidler. 2006. Passive sexual transmission of human immunodeficiency virus type 1 variants and adaptation in new hosts. J. Virol. **80:**7226–7234.

14. **Friedrich, T. C., E. J. Dodds, L. J. Yant, L. Vojnov, R. Rudersdorf, C. Cullen, D. T. Evans, R. C. Desrosiers, B. R. Mothe, J. Sidney, A. Sette, K. Kunstman, S. Wolinsky, M. Piatak, J. Lifson, A. L. Hughes, N. Wilson, D. H. O'Connor, and D. I. Watkins.** 2004. Reversion of CTL escape-variant immunodeficiency viruses in vivo. Nat. Med. **10:**275–281.
15. **Friedrich, T. C., C. A. Frye, L. J. Yant, D. H. O'Connor, N. A. Kriewaldt, M. Benson, L. Vojnov, E. J. Dodds, C. Cullen, R. Rudersdorf, A. L. Hughes, N. Wilson, and D. I. Watkins.** 2004. Extraepitopic compensatory substitutions partially restore fitness to simian immunodeficiency virus variants that escape from an immunodominant cytotoxic-T-lymphocyte response. J. Virol. **78:**2581–2585.
16. **Ganusov, V. V., and R. J. De Boer.** 2006. Estimating costs and benefits of CTL escape mutations in SIV/HIV infection. PLoS Comput. Biol. **2:**e24.
17. **Goulder, P. J., and D. I. Watkins.** 2004. HIV and SIV CTL escape: implications for vaccine design. Nat. Rev. Immunol. **4:**630–640.
18. **Goulder, P. J. R., R. E. Phillips, R. A. Colbert, S. McAdam, G. Ogg, M. A. Nowak, P. Giangrande, G. Luzzi, B. Morgan, A. Edwards, A. J. McMichael, and S. Rowland-Jones.** 1997. Late escape from an immunodominant cytotoxic T-lymphocyte response associated with progression to AIDS. Nat. Med. **3:**212–217.
19. **Harcourt, G. C., S. Garrard, M. P. Davenport, A. Edwards, and R. E. Phillips.** 1998. HIV-1 variation diminishes CD4 T lymphocyte recognition. J. Exp. Med. **188:**1785–1793.
20. **Jones, N. A., X. Wei, D. R. Flower, M. Wong, F. Michor, M. S. Saag, B. H. Hahn, M. A. Nowak, G. M. Shaw, and P. Borrow.** 2004. Determinants of human immunodeficiency virus type 1 escape from the primary CD8+ cytotoxic T lymphocyte response. J. Exp. Med. **200:**1243–1256.
21. **Kent, S. J., C. S. Fernandez, C. Jane Dale, and M. P. Davenport.** 2005. Reversion of immune escape HIV variants upon transmission: insights into effective viral immunity. Trends Microbiol. **13:**243–246.
22. **Leslie, A. J., K. J. Pfafferott, P. Chetty, R. Draenert, M. M. Addo, M. Feeney, Y. Tang, E. C. Holmes, T. Allen, J. G. Prado, M. Altfeld, C. Brander, C. Dixon, D. Ramduth, P. Jeena, S. A. Thomas, A. S. John, T. A. Roach, B. Kupfer, G. Luzzi, A. Edwards, G. Taylor, H. Lyall, G. Tudor-Williams, V. Novelli, J. Martinez-Picado, P. Kiepiela, B. D. Walker, and P. J. Goulder.** 2004. HIV evolution: CTL escape mutation and reversion after transmission. Nat. Med. **10:**282–289.
23. **Loh, L., C. J. Batten, J. Petravic, M. P. Davenport, and S. J. Kent.** 2007. In vivo fitness costs of different Gag CD8 T-cell escape mutant simian-human immunodeficiency viruses for macaques. J. Virol. **81:**5418–5422.
24. **Loh, L., J. Petravic, C. J. Batten, M. P. Davenport, and S. J. Kent.** Vaccination and timing influence SIV immune escape viral dynamics in vivo. PLoS Pathog. **4:**e12.
25. **Mandl, J. N., R. R. Regoes, D. A. Garber, and M. B. Feinberg.** 2007. Estimating the effectiveness of simian immunodeficiency virus-specific CD8+ T cells from the dynamics of viral immune escape. J. Virol. **81:**11982–11991.
26. **Marée, A. F., W. Keulen, C. A. Boucher, and R. J. De Boer.** 2000. Estimating relative fitness in viral competition experiments. J. Virol. **74:**11067–11072.
27. **Martinez-Picado, J., J. G. Prado, E. E. Fry, K. Pfafferott, A. Leslie, S. Chetty, C. Thobakgale, I. Honeyborne, H. Crawford, P. Matthews, T. Pillay, C. Rousseau, J. I. Mullins, C. Brander, B. D. Walker, D. I. Stuart, P. Kiepiela, and P. Goulder.** 2006. Fitness cost of escape mutations in p24 Gag in association with control of human immunodeficiency virus type 1. J. Virol. **80:**3617–3623.
28. **Moore, C. B., M. John, I. R. James, F. T. Christiansen, C. S. Witt, and S. A. Mallal.** 2002. Evidence of HIV-1 adaptation to HLA-restricted immune responses at a population level. Science **296:**1439–1443.
29. **Nature.** 2007. HIV vaccine failure prompts Merck to halt trial. Nature **449:**390.
30. **Nishimura, Y., T. Igarashi, O. K. Donau, A. Buckler-White, C. Buckler, B. A. Lafont, R. M. Goeken, S. Goldstein, V. M. Hirsch, and M. A. Martin.** 2004. Highly pathogenic SHIVs and SIVs target different CD4+ T cell subsets in rhesus monkeys, explaining their divergent clinical courses. Proc. Natl. Acad. Sci. USA **101:**12324–12329.
31. **Nowak, M. A., A. L. Lloyd, G. M. Vasquez, T. A. Wiltrout, L. M. Wahl, N. Bischofberger, J. Williams, A. Kinter, A. S. Fauci, V. M. Hirsch, and J. D. Lifson.** 1997. Viral dynamics of primary viremia and antiretroviral therapy in simian immunodeficiency virus infection. J. Virol. **71:**7518–7525.
32. **Phillips, R. E., S. Rowland-Jones, D. F. Nixon, F. M. Gotch, J. P. Edwards, A. O. Ogunlesi, J. G. Elvin, J. A. Rothbard, C. R. M. Bangham, C. R. Rizza, and A. J. McMichael.** 1991. Human immunodeficiency virus genetic variation that can escape cytotoxic T cell recognition. Nature **354:**453–459.
33. **Ribeiro, R. M., M. D. Hazenberg, A. S. Perelson, and M. P. Davenport.** 2006. Naive and memory cell turnover as drivers of CCR5-to-CXCR4 tropism switch in human immunodeficiency virus type 1: implications for therapy. J. Virol. **80:**802–809.
34. **Richman, D. D., T. Wrin, S. J. Little, and C. J. Petropoulos.** 2003. Rapid evolution of the neutralizing antibody response to HIV type 1 infection. Proc. Natl. Acad. Sci. USA **100:**4144–4149.
35. **Schwartz, E. J., A. U. Neumann, A. V. Teixeira, L. A. Bruggeman, J. Rappaport, A. S. Perelson, and P. E. Klotman.** 2002. Effect of target cell availability on HIV-1 production in vitro. AIDS **16:**341–345.
36. **Wei, X., J. M. Decker, S. Wang, H. Hui, J. C. Kappes, X. Wu, J. F. Salazar-Gonzalez, M. G. Salazar, J. M. Kilby, M. S. Saag, N. L. Komarova, M. A. Nowak, B. H. Hahn, P. D. Kwong, and G. M. Shaw.** 2003. Antibody neutralization and escape by HIV-1. Nature **422:**307–312.
37. **Wilson, D. P., J. J. Mattapallil, M. D. Lay, L. Zhang, M. Roederer, and M. P. Davenport.** 2007. Estimating the infectivity of CCR5-tropic simian immunodeficiency virus SIV_{mac251} in the gut. J. Virol. **81:**8025–8029.
38. **Yu, X. G., M. M. Addo, E. S. Rosenberg, W. R. Rodriguez, P. K. Lee, C. A. Fitzpatrick, M. N. Johnston, D. Strick, P. J. Goulder, B. D. Walker, and M. Altfeld.** 2002. Consistent patterns in the development and immunodominance of human immunodeficiency virus type 1 (HIV-1)-specific CD8+ T-cell responses following acute HIV-1 infection. J. Virol. **76:**8690–8701.
39. **Zhang, Z. Q., S. W. Wietgrefe, Q. Li, M. D. Shore, L. Duan, C. Reilly, J. D. Lifson, and A. T. Haase.** 2004. Roles of substrate availability and infection of resting and activated CD4+ T cells in transmission and acute simian immunodeficiency virus infection. Proc. Natl. Acad. Sci. USA **101:**5640–5645.